

Zigzag spin chains with antiferromagnetic-ferromagnetic interactions: Transfer-matrix renormalization group study

H. T. Lu,^{1,2} Y. J. Wang,³ Shaojin Qin,² T. Xiang²

¹*School of Physics, Peking University, Beijing 100871, China*

²*Institute of Theoretical Physics and Interdisciplinary Center of Theoretical Studies, Chinese Academy of Sciences, Beijing 100080, China*

³*Department of Physics, Beijing Normal University, Beijing 100875, China*

(Dated:)

Properties of the zigzag spin chains with various nearest-neighbor and next-nearest-neighbor interactions are studied by making use of the transfer-matrix renormalization group method. Thermodynamic quantities of the systems (temperature dependence of the susceptibility and the specific heat), as well as the field dependence of the magnetization are analyzed numerically with a high accuracy in the thermodynamic limit. The results have been compared with the recent experimental data on $\text{Rb}_2\text{Cu}_2\text{Mo}_3\text{O}_{12}$.

PACS numbers: 75.10.Jm, 75.40.Cx, 75.40.Mg

I. INTRODUCTION

Spin models with charge degrees of freedom frozen, as an effective low-energy description for insulating systems, have been proved to be a fruitful resource of fundamental concepts and principles in condensed matter physics and other related fields. Besides theoretical explorations, advanced probe tools and measurements, combined with multifarious natural and artificial materials, such as ceramic or organic compounds, and optical lattices provide remarkable practical platforms for theoretical investigations. The simplest one-dimensional (1D) quantum spin model is the nearest-neighbor (NN) Heisenberg model:

$$H = J \sum_i \mathbf{S}_i \cdot \mathbf{S}_{i+1}, \quad (1)$$

where \mathbf{S}_i is the quantum spin operator. From Bethe's seminal paper¹ and successive works, we know that the ground state of a spin- $\frac{1}{2}$ antiferromagnetic (AF) ($J > 0$) chain is a singlet ($\mathbf{S}_{\text{tot}} = 0$) and has quasi-long-range order with algebraically decaying spin correlations. The gapless spectrum contains no single-particle excitations and is instead a continuum of states. The elementary excitations are called spinons, which carry spin 1/2 and appear only in pairs in all physical states with integer total spin. This picture is qualitatively different from the prediction of a spin-wave theory, which is usually effective in higher-dimensional systems. The gapless behavior is special for half-integer Heisenberg spin chains, while for integer ones, Haldane conjectured that there exists a finite gap.² Experimental, numerical, and theoretical studies have confirmed this conjecture for $S = 1$ and some other higher spin values.³ On the other hand, half-integer spin chains can be driven to a gapped phase by frustrations. Throughout this paper, we confine our discussions to the spin-1/2 case.

A straightforward generalization of the NN Heisenberg model is to include the next-nearest-neighbor (NNN) in-

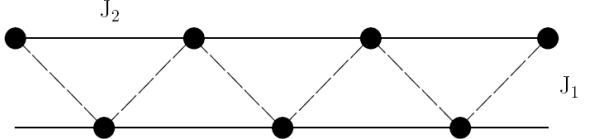


FIG. 1: Heisenberg zigzag spin chains.

teractions:

$$H = \sum_{i=1}^N (J_1 \mathbf{S}_i \cdot \mathbf{S}_{i+1} + J_2 \mathbf{S}_i \cdot \mathbf{S}_{i+2}), \quad (2)$$

where J_1 or J_2 is NN or NNN exchange interaction constant, and periodic boundary conditions are implied. This is usually called the J_1 - J_2 model, which can be also considered as a model for a zigzag spin chain, as shown in Fig. 1.

The J_1 - J_2 model has been investigated theoretically over the decades. With $J_2 > 0$, it is a frustrated (competing) system, irrespective of the sign of J_1 . When $J_1 > 0$ and $J_2 > 0$ (AF-AF), the ground state is a spin liquid. The increase of the ratio of the coupling constants $\alpha (\equiv J_2/J_1)$ induces an infinite-order phase transition from a gapless state to a gapful dimerized state.^{4,5} The critical point α_c is numerically estimated to be ≈ 0.241 .⁶ When α is further increased to the so-called Majumdar-Ghosh (MG) point at 1/2, the ground state is the products of singlet pairs formed by nearest neighboring spins.^{7,8} It is two-fold degenerate since the Z_2 symmetry of translations by one site is spontaneously broken. When $J_1 < 0$ and $J_2 > 0$ (F-AF) with $-1/4 < \alpha \leq 0$, the ground state is fully ferromagnetic (FM), and becomes an ($S = 0$) incommensurate state for $\alpha < -1/4$.⁹ It is suggested that in this incommensurate state the gap is strongly suppressed.¹⁰ For $\alpha = -1/4$, the exact ground state can be shown¹¹ to have a ($N + 2$)-fold degeneracy, comprised by $S = 0$ and $S = N/2$ states (with N the lattice size). When $J_1 > 0$ and $J_2 < 0$ (AF-F), the system

is believed to be in a gapless antiferromagnetic phase for any permissible values of J_1 and J_2 .

There are many papers contributing to the AF-AF case and the related extended models. The other two cases (F-AF and AF-F), although having caught relatively less attention, also show very interesting phenomena, which we will mainly deal with in this paper. Aside from the general aspect of theoretical interest, especially for understanding the roles played by frustration and incommensurability, an additional motivation to study this system lies in the fact that physically, it is believed that a large class of copper oxides can be essentially described by the J_1 - J_2 model.

Copper oxides are excellent model systems for low dimensional spin- $\frac{1}{2}$ quantum magnets, where magnetic Cu^{2+} ions carry 1/2 spins. The basic building blocks are CuO_4 plaquettes and there are three ways of linking these fundamental units. One is adjacent squares sharing their corners, as shown in (a) of Fig. 2. A typical example is Sr_2CuO_3 . These corner-sharing chains can expand in the plane to form a CuO_2 sheet, constituting the basic structure in cuprates. The dominant interaction in a corner-sharing chain is the NN superexchange. Linear Cu-O-Cu bonds along the spin chains give rise to a large antiferromagnetic NN exchange coupling. As in Sr_2CuO_3 , the NN coupling constant is estimated to be 2100 ± 200 K.¹² The second kind is edge-sharing, as shown in Fig. 2 (b). Because of the nearly 90° Cu-O-Cu bond in the edge-sharing squares, an $\text{O}2p_\sigma$ orbital hybridizing with a $3d$ orbital of Cu ion is almost orthogonal to that of the next Cu ion. The NN interaction J_1 can vary from antiferromagnetic to ferromagnetic, as the angle θ of the Cu-O-Cu bond approaches 90° from a larger value.¹³ This nearly orthogonality makes the NN coupling in the edge-sharing case more than an order of magnitude smaller than the corner-sharing. The sign and the absolute value of the

NN interaction depend sensitively on the bond angle θ and the distance between copper and oxygen ions. We refer readers to Table I of Ref. 14 for details. The third configuration is the combination of corner-sharing and edge-sharing in one spin chain simultaneously, such as in SrCuO_2 , as shown in Fig. 2 (d). In SrCuO_2 , the NNN coupling, which is the superexchange interaction through the linear Cu-O-Cu, is almost ten times greater than the NN one through sharing the edges.¹⁵

In corner-sharing chains, the NNN interaction can often be neglected safely due to its small magnitude relative to the NN interaction. For the edge-sharing case, the situation is quite different. The NNN interaction J_2 through the Cu-O-O-Cu path is generally antiferromagnetic, usually with a magnitude of a few tens Kelvin. Despite its smallness, J_2 has a pronounced effect on the physical properties of these systems since the NN coupling is also small. Therefore, edge-sharing copper oxides provide abundant experimental materials for studying the zigzag spin chain model, which can cover a large region of the parameter space.

On the other hand, at low temperatures, besides intrachain couplings J_1 and J_2 , other forms of interactions often become relevant, driving a system to various phases with the decrease of temperature. For example, spin-phonon interactions can induce a spin-Peierls instability, as in CuGeO_3 .¹⁶ If interchain interactions are strong enough, an antiferromagnetically long-ranged order will appear below the Néel temperature T_N , as in $\text{Ca}_2\text{Y}_2\text{Cu}_5\text{O}_{10}$,¹⁷ $\text{La}_6\text{Ca}_8\text{Cu}_{24}\text{O}_{41}$,¹⁸ and Li_2CuO_2 .¹⁹ Another interesting case is LiCu_2O_2 ,²⁰ which undergoes a transition to a magnetic helix state at low temperatures. By a comparative study on the similar oxide NaCu_2O_2 , it has been shown that interchain interactions over a few chains should be incorporated to explain the experimental results.²¹ These facts reveal the complexity of the interactions underlying edge-sharing copper oxides at low temperatures.

Since the effect of NNN interaction is important for edge-sharing copper oxide chains, the study on the J_1 - J_2 model not only has its own theoretical meaning, but also obtains a connection with practical materials. In this paper, in the thermodynamic limit and extending to the low-temperature region, we use the transfer-matrix renormalization group (TMRG) method^{22,23,24} to study the thermodynamic properties of the J_1 - J_2 model with antiferromagnetic-ferromagnetic interactions.

The TMRG is a powerful numerical tool for studying the thermodynamic properties of 1D quantum systems. It starts by expressing the partition function as a trace on the product of the transfer matrix \mathcal{T}_M using the Trotter-Suzuki decomposition.

$$Z = \text{Tr}e^{-\beta H} = \lim_{M \rightarrow \infty} \text{Tr}\mathcal{T}_M^{N/2}, \quad (3)$$

where M is the Trotter number, and N is the total cell number in the lattice, $\tau = \beta/M$. The definition of \mathcal{T}_M can be found from Refs. 22,23,24. For the J_1 - J_2 model

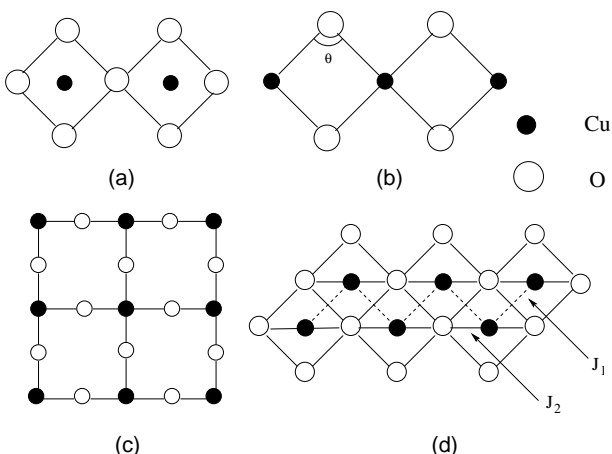


FIG. 2: Various ways of linking CuO_4 plaquettes. (a) The corner-sharing chain, as in Sr_2CuO_3 ; (b) the edge-sharing chain, as in CuGeO_3 , Li_2CuO_2 , and $\text{Rb}_2\text{Cu}_2\text{Mo}_3\text{O}_{12}$; (c) CuO_2 plane expanded by corner-sharing chains, as in cuprates; (d) the zigzag chain in SrCuO_2 .

considered here, each cell consists of two adjoining spins. In the thermodynamic limit $N \rightarrow \infty$, the free energy f , internal energy u , and uniform magnetization m_z can be expressed by the maximum eigenvalue λ_{\max} and the corresponding left $\langle \psi^L |$ and right $| \psi^R \rangle$ eigenvectors of the transfer matrix \mathcal{T}_M :

$$f = -\lim_{N \rightarrow \infty} \frac{1}{N\beta} \ln Z = -\frac{1}{2\beta} \lim_{M \rightarrow \infty} \ln \lambda_{\max}, \quad (4)$$

$$u = \frac{\langle \psi^L | \tilde{\mathcal{T}}_U | \psi^R \rangle}{\lambda_{\max}}, \quad (5)$$

$$m_z = \frac{\langle \psi^L | \tilde{\mathcal{T}}_M | \psi^R \rangle}{\lambda_{\max}}, \quad (6)$$

where the definition of the transfer matrices $\tilde{\mathcal{T}}_U$ and $\tilde{\mathcal{T}}_M$, which are similar to \mathcal{T}_M , can also be found in Refs. 22, 23,24. The specific heat and magnetic susceptibility can then be calculated by numerical derivatives of u and m_z , respectively,

$$C = \frac{\partial u}{\partial T}, \quad (7)$$

$$\chi = \frac{\partial m_z}{\partial H}. \quad (8)$$

In our numerical simulation, $\tau = 0.05$, the error caused by the Trotter-Suzuki decomposition is less than 10^{-3} . During the TMRG iterations, 60–80 states are retained and the truncation error is less than 10^{-4} down to $k_B T \sim 0.01J$.

The outline of this paper is as follows: Section II and Sec. III are devoted to discussions on F-AF and AF-F cases, respectively. Section IV shows our numerical results compared with the newly experiments on $\text{Rb}_2\text{Cu}_2\text{Mo}_3\text{O}_{12}$.¹⁴ We conclude with a brief summary in Sec. V.

II. THE F-AF CASE

As mentioned in the previous section, at the critical point $\alpha_c = -1/4$, two distinct configurations with the energy $E_g = -3N|J_1|/16$ are the ground states, where N is the lattice size.¹¹ One is fully ferromagnetic with $S_{\text{tot}} = N/2$, the other is a singlet state with $S_{\text{tot}} = 0$. The state vector for the latter can be expressed as

$$\Phi = \sum [i, j] [k, l] [m, n] \dots,$$

where the summation is made for any combination of spin sites under the condition that $i < j$, $k < l$, $m < n$, \dots , and $[i, j]$ denotes the singlet pair. This is also called a uniformly distributed resonant-valence-bond (UDRVB) state.

In the region $0 \geq \alpha > -1/4$, the ground state lies in the subspace $\mathbf{S}_{\text{tot}} = N/2$ with the degeneracy $N + 1$. The ground state energy $E_g = -N|J_1|(1 + \alpha)/4$. For $\alpha < -1/4$, the ground state lies in the subspace $\mathbf{S}_{\text{tot}} = S_{\text{tot}}^z =$

0 and the lattice translational symmetry is thought to be broken. For the critical point $\alpha_c = -1/4$, besides the ferromagnetic configuration, the UDRVb state restores the lattice translational symmetry.

When $\alpha < -1/4$, whether the system is gapped or gapless is an interesting and controversial issue. When $J_2 \gg |J_1|$, it is appropriate to regard the model as two antiferromagnetic spin chains coupled by a weak zigzag interchain interaction J_1 . This coupling can be expressed by the current-current interaction^{5,25} in terms of the Wess-Zumino-Witten fields (see, e.g., Ref. 26). If $J_1 > 0$, by renormalization group (RG) analysis, this interaction is marginally relevant and produces an exponentially small gap $\Delta \propto \exp(-\text{const}J_2/J_1)$, which leads to a spontaneously dimerized ground state.^{5,25} While at the ferromagnetic side, i.e. $J_1 < 0$, the model was believed to be gapless because the current-current interaction renormalizes logarithmically to zero.⁵ It was conjectured that the ferromagnetic model is critical with different velocities for the spin-singlet and spin-triplet excitations.²⁵ Afterward, Nersesyan *et al.*²⁷ found that in addition to the current-current interaction, a “twist” term associated with the staggered component of the spin operators arises in the zigzag chains. Due to this parity-breaking term, the critical point $J_1 = 0$ is unstable both in the ferromagnetic ($J_1 < 0$) and antiferromagnetic ($J_1 > 0$) regions.^{27,28}

The phase diagram for the F-AF model in an external magnetic field was discussed by Chubukov.²⁹ In addition to the ferromagnetic phase, two different biaxial and uniaxial spin nematic phases are mapped out. In these nematiclike phases there is an extra symmetry breaking of reflections about a bond or about a site. In the absence of external field, with the decrease of α starting from $-1/4$, the system develops from the chiral biaxial spin nematic phase to the dimerized uniaxial spin nematic phase at $\alpha \simeq -0.385$. The Lieb-Schultz-Mattis theorem³⁰ states that a half-integer spin chain with essentially any reasonably local Hamiltonian respecting translational and rotational symmetries either has a zero gap (i.e. “mass”) or else has degenerate ground states, corresponding to a spontaneously broken parity. If the phase diagram is correct, we could expect an energy gap at $\alpha < -1/4$.

On the other hand, numerical analysis has shown a complicated size dependence of the ground-state energy and correlation function in the region $\alpha < -1/4$.^{9,31} This phenomenon, combined with the fact of slow convergence and no detection of energy gap at the resolution of the numerical simulations indicates an unusually long correlation length in the F-AF chain.

By taking into account the twist term, the RG analysis¹⁰ found that although the unstable RG flow around the critical point $J_1 = 0$ produces an energy gap in the ferromagnetic coupling as well as the antiferromagnetic one, in the ferromagnetic side, due to the existence of a marginally relevant fixed line, the gap is strongly reduced. In an extended region for the J_1 of order one, the correlation length can be extremely large and the gap, if exists, is so strongly suppressed that numerical methods

can not detect it.

Another closely related topic worth mentioning is the incommensurability in the zigzag spin chains. For simple antiferromagnetic Heisenberg spin-1/2 chains and ladders, the well known mechanisms for generating incommensurabilities are via external magnetic fields or Dzyaloshinskii-Moria interaction. While in the zigzag spin chain, it has been found that the frustrated interaction $J_2 > 0$ can also produce incommensurability.^{5,31}

In classical picture, by regarding spin operators \mathbf{S}_i as classical vectors, the energy per site can be expressed as

$$E(\theta) = J_1 \cos \theta + J_2 \cos 2\theta \quad (9)$$

for Hamiltonian (2). The pitch angle is given by

$$\cos \theta = -J_1/4J_2 \quad (10)$$

for $|\alpha| = |J_2/J_1| \geq 1/4$. As $J_1 > 4J_2 \geq 0$, $\theta = \pi$; $-J_1 > 4J_2 \geq 0$, $\theta = 0$. At the special point $J_1 = 0$, $\theta = \pi/2$, and the deviations from the normal values (π for the AF-AF case and 0 for the F-AF) begin to occur at $|\alpha| = 1/4$. In quantum level, the characteristic momentum Q of the spin-spin correlation function which maximizes the static structure factor is either π or 0, corresponding to the antiferromagnetic or ferromagnetic spin chain with $J_2 = 0$, respectively. With the increase of J_2 , Q departs from its usual value. Numerical simulations^{5,31} display that for the AF-AF case, Q deviates from π with the increase of J_2 after crossing the MG point ($J_2 = J_1/2$) where the dimerization has already taken place. On the other side, the departure of Q from 0 sets in at the critical point $J_2 = -J_1/4$ for the F-AF case. This asymmetry may be understood on account of the effects of the current-current interaction and the twist term.

It was shown that in the presence of exchange anisotropic, the twist term induces incommensurabilities in the spin correlations.²⁷ We have reason to expect this to hold true even in the SU(2) symmetric (i.e. isotropic) case.^{32,33} In the AF-AF isotropic case, both the twist term and the current-current interaction diverge simultaneously to reach the strong coupling phase as the RG flows to $J_2 \gg J_1$.³² The pure current-current interaction induces massive spinons which can be regarded as quantum dimerization kinks, driving the zigzag spin chain into the dimerized phase. The twist term appearing in the zigzag case is merely to shift the minimum of the two-spinon continua to incommensurate wave numbers, which does not alter the massive spinon picture qualitatively.³² If these two terms become relevant at different points, we may observe the emergence of dimerization and incommensurability one after the other, as in the AF-AF case. For the F-AF case, the current-current interaction is marginally irrelevant since it renormalizes logarithmically to zero.⁵ The twist term becomes dominative. We can observe the incommensurability only, and hardly detect the gap following with the dimerization. But there is not a simple way to separate the effects of the current-current and twist interactions in the isotropic zigzag spin

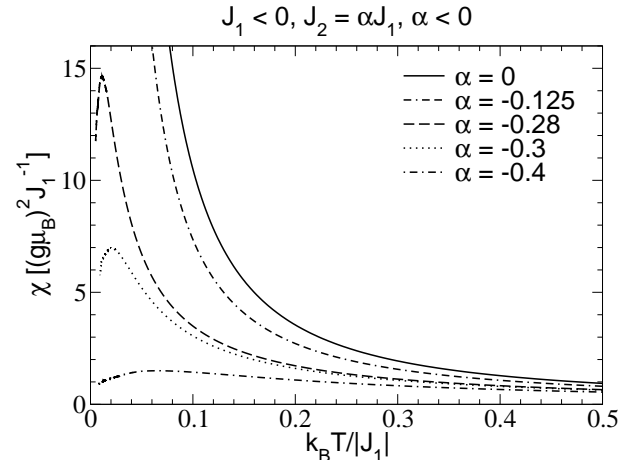


FIG. 3: Temperature dependence of the uniform susceptibility at various α for the F-AF case.

chains as in the anisotropic ones. There is still much theoretical work to be accomplished.

Since the TMRG gives results for observable quantities in the thermodynamic limit, we are able to exploit it to study the bulk properties of the system without worrying the finite size effect. The complicated size dependence of the ground-state energy and correlation function found in the region $\alpha < -1/4$ (Refs.^{9,31}) may be avoided.

Figures 3 and 4 show the TMRG results on the temperature dependence of the susceptibility χ , specific heat C , and heat coefficient C/T at various α for the F-AF case. At $\alpha = 0$, the model reduces to the case of ferromagnetic spin chain. The curves of $\alpha = 0$ describe the properties of χ and C for a ferromagnetic spin chain, which behave in the low temperature limit:

$$\begin{aligned} \chi &\sim T^{-2}, \\ C &\sim \sqrt{T}. \end{aligned}$$

At $\alpha > -1/4$, the temperature dependence of χ always diverges, indicating that the system lies in a ferromagnetic state. At the critical point $\alpha = -1/4$, a phase transition from the ferromagnetic state to the singlet state takes place. In the region $\alpha < -1/4$, remarkable suppressions of the susceptibility can be observed, and with the decrease of α , the peaks of χ move to higher temperatures with its heights decreased rapidly.

For the temperature dependence of the specific heat, the most remarkable feature is the development of a double-peak structure. With the decrease of α , at intermediate temperatures, a broad maximum is maintained and its height lowered. A relatively sharp peak at low temperatures, induced by the NNN AF interaction J_2 , appears and develops, and its position moves to higher temperatures. We expect that this peak would approach the maximum of $C(T)$ for a pure AF Heisenberg chain.³⁴ The drastic change on the shape of the curves between $\alpha = -0.125$ and $\alpha = -0.28$ implies a phase transition.

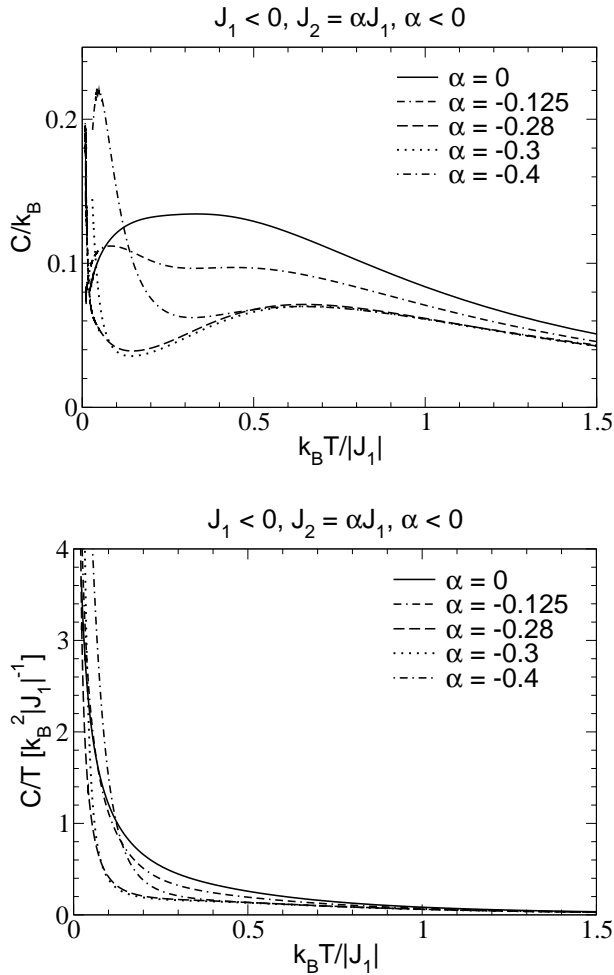


FIG. 4: The specific heat C and heat coefficient C/T at various α for the F-AF case.

The similar double-peak structure for the J_1 - J_2 model in the F-AF case has also been found in Ref. 35. By applying a method of hierarchy of algebras, the authors calculated thermodynamic quantities of the linear ring of size 16 described by the same model (2). Our results are qualitatively in agreement with theirs. Recently, this double-peak structure in the specific heat for the moderate value $\alpha = -1/3$ has also been confirmed by exact diagonalization methods.³⁶ Furthermore, for various α we have considered, C/T as a function of T decreases monotonously down to $T \sim 0.03$. This fact reflects a high density of low-excitation states in this region, and confirms the results obtained from the density-matrix renormalization group calculations.¹⁰

From the numerical results above, we find that the existence of gap near the critical point α_c is still a question. The behaviors of susceptibility and specific heat indicate that if a gap exists near $\alpha < -1/4$, it should be very small. The properties of the excitations near and far from α_c need to be investigated further.

III. THE AF-F CASE

In the AF-F case with $J_1 > 0$ and $J_2 < 0$, the behavior of the zigzag spin chain is believed to be antiferromagnetic with no gap for any permissible values of J_1 and J_2 .³¹ The arguments are based on a simple spin-wave analysis. The spectrum of spin-wave excitations is given by

$$\epsilon_k = 2S\sqrt{\lambda_k^2 - \gamma_k^2}, \quad (11)$$

where $S = 1/2$, $\alpha = J_2/J_1 < 0$, $\lambda_k = -2\alpha \sin^2 k + 1$, $\gamma_k = \cos k$. ϵ_k is linear as $k \rightarrow 0$:

$$\epsilon_k \sim vk \quad (12)$$

with $v = 2S\sqrt{-4\alpha + 1}$. Although the spin-wave theory is not quite correct for antiferromagnetic spin chains, it is still insightful in shedding light on the qualitative picture of the excitations around the characteristic momentum $k = 0, \pi$. We see that for the AF-F case, there also exist gapless excitations at $k = 0, \pi$.

According to Lieb's discussion,³⁷ Hamiltonian (2) with $J_1 > 0, J_2 < 0$ describes spin systems at a bipartite lattice. The absolute ground state of the AF-F spin chain should lie in the $\mathbf{S} = 0$ sector. On the other hand, the relative ground state in each subspace $V(M)$ of the total magnetic quantum number M is unique. Thus we deduce that the absolute ground state in the AF-F case is nondegenerate. The Lieb-Schultz-Mattis theorem asserts that for a half-integer spin chain with reasonably local Hamiltonian respecting translational and rotational symmetries, either the parity is spontaneously broken in the ground state or else there are gapless excitations of odd parity, under the condition that the ground state is rotational invariant.³⁰ Combining these two statements, we expect the system should be gapless.

It is not trivial to make the above statement completely rigorous, considering the relative ground state in the subspaces $V(M)$ may not be unique in the thermodynamic limit $N \rightarrow \infty$. In order to confirm the conclusion, we calculate the temperature dependence of the susceptibility and specific heat for various α by using the TMRG method.

Figures 5 and 6 show the TMRG results on the temperature dependence of the susceptibility χ , specific heat C , and heat coefficient C/T at various α for the AF-F case. With the decrease of α , the behaviors of χ and C do not change qualitatively. $\chi \rightarrow \text{const}$ (nonzero) and $C \sim T$ as $T \rightarrow 0$. The Bonner-Fisher peak in $\chi(T)$ (Ref.³⁸) moves to higher T with the decrease of α . Phase transition is not observed. The slopes of C , or the intersections of C/T at zero temperature (shown in Fig. 6) decrease with the decrease of α . This indicates that the density of low-excitation states becomes smaller and the spin fluctuations are suppressed by the NNN FM interaction.

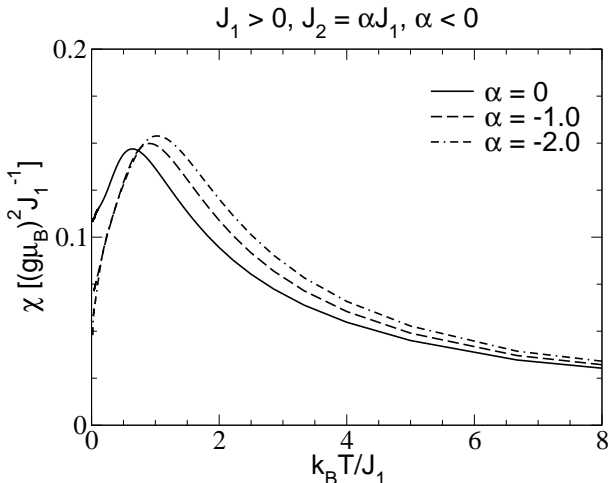


FIG. 5: Temperature dependence of the uniform susceptibility at various α for the AF-F case.

IV. COMPARISON WITH THE EXPERIMENTAL RESULTS

In the previous two sections, we have discussed thermodynamic properties of the J_1 - J_2 model for the F-AF and AF-F cases and our numerical results cover their whole phases. In experiments, in order to understand the physics of edge-sharing copper chains, it is important to determine both sign and magnitude of NN and NNN interaction coefficients. One way for this purpose is to measure thermodynamic quantities, such as specific heat, susceptibility and magnetization, together with numerical fitting on these data. Such a method has been widely used in the studies on copper chains and its efficiency has been proved, such as in SrCuO_2 ,¹⁵ NaCu_2O_3 ,²¹ $\text{Ca}_2\text{Y}_2\text{Cu}_5\text{O}_{15}$,¹⁷ and $\text{La}_6\text{Ca}_8\text{Cu}_{24}\text{O}_{41}$.¹⁸

Recently, the magnetic susceptibility and magnetization of the edge-sharing copper oxide $\text{Rb}_2\text{Cu}_2\text{Mo}_3\text{O}_{12}$ (Ref.³⁹) have been measured.¹⁴ The most interesting finding is that no magnetic phase transition was observed down to 2 K. Therefore, the compound is suitable for studying the properties of the ground state of the J_1 - J_2 model. It was proposed that at first approximation, it could be described by a F-AF J_1 - J_2 model.¹⁴ We have known that for the F-FA chain, the unusually long correlation length, which exist even at high-frustrated region, can lead to prominent finite-size effect for the usual cluster simulations. Therefore, as a primary step, reliable numerical results on thermodynamic quantities free of finite-size effect on the pure J_1 - J_2 model may be essential in making a quantitative comparison between experimental and theoretical studies. In this section, we use the TMRG method to simulate the experimental results based on model (2).

The strategy is as follows: For a fixed α , we first use the TMRG to calculate the temperature dependence of the

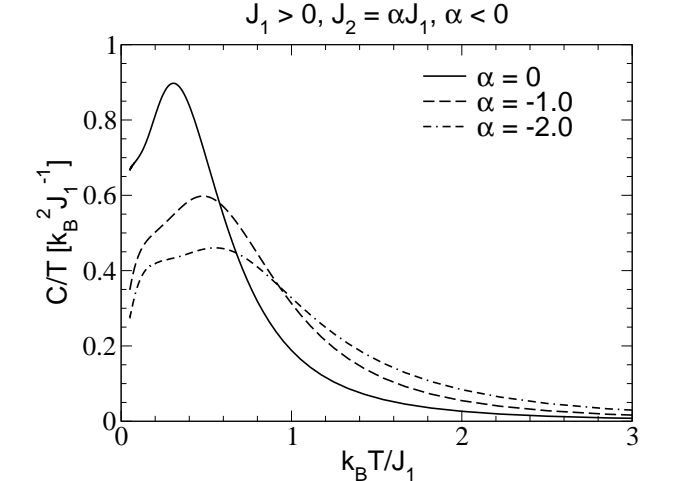
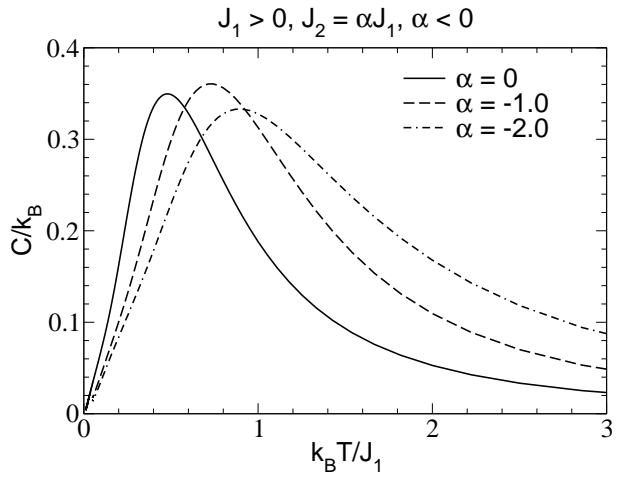


FIG. 6: The specific heat C and heat coefficient C/T at various α for the AF-F case.

susceptibility in the units of J_1 . Then, according to the position of the peak in the numerical result and the actual value obtained in the experiment, we can determine the value J_1 uniquely, on the condition that the calculated peak's position coincides with the experiment. The g value is taken to be 2.03 as in Ref. 14. The following is what we observed.

For the AF-AF case (Fig. 7), the height of the peak decreases with the increase of α . The possibility for this type of interaction can be excluded.

For the F-AF case (Fig. 8), we see that with α approaching the critical point $-1/4$, to keep the peak position unchanged, the magnitude of J_1 acquires a value of thousands of Kelvin. Furthermore, the deviation from the experiment data at high temperatures becomes more conspicuous. While taking the parameters $J_1 = -138$ K and $\alpha = -0.37$ as in Ref. 14, the temperature for the peak is less than $T_{\max} = 14.3$ K found in the experiment. Besides, for $\alpha < -0.5$, a broad peak located at $T \sim J_2$ in the temperature dependence of susceptibility emerges, which is a characteristic feature of one-dimensional Heisenberg

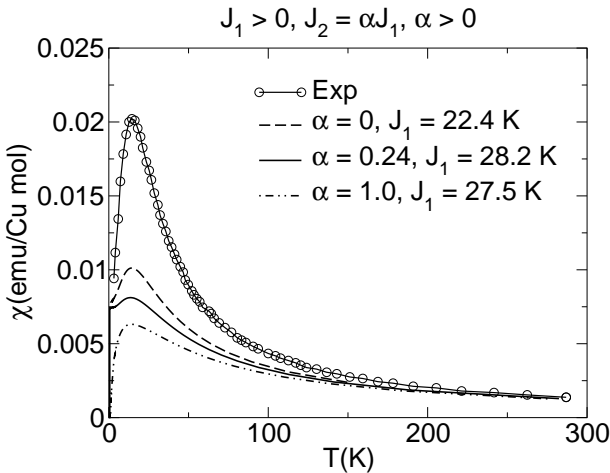


FIG. 7: Comparison of the TMRG results for the susceptibility in the AF-AF case with the experimental measurement in Ref. 14.

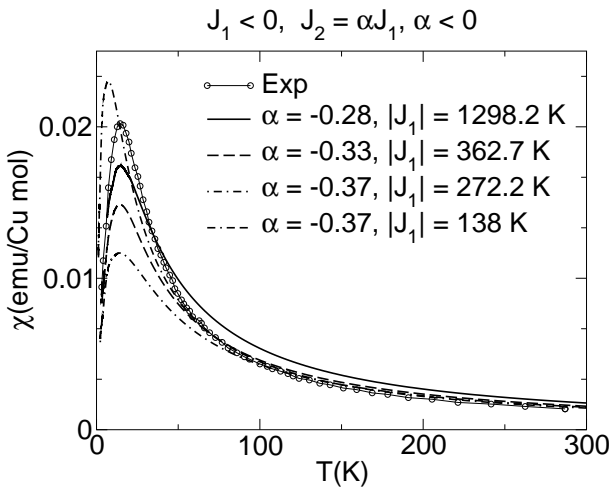


FIG. 8: Comparison of the TMRG results for the susceptibility in the F-AF case with the experimental measurement in Ref. 14.

antiferromagnetic chain.³⁸ This suggests that the antiferromagnetic component becomes significant for larger α . However, we failed to obtain a satisfactorily stable result below the peak temperature when $\alpha < -1$.

For the AF-F case (Fig. 9), at $J_1 = 12.31$ K and $\alpha = -3.5$, the numerical result seems to fit the experiment data rather well, except for a little deviation in the left side of the peak at low temperatures. But there are several questionable points remained. According to the analysis of Mizuno et al¹³, the NNN interaction through Cu-O-O-Cu should be antiferromagnetic, i.e. $J_2 > 0$. However, the interactions of AF-F type may also be a candidate. In Ref. 40, Matsuda and coworkers proposed a model to explain the anomalous magnetic excitations in the edge-sharing CuO₂ chains of La₅Ca₉Cu₂₄O₄₁. The intra- and interchain interactions are of AF-F type. (See

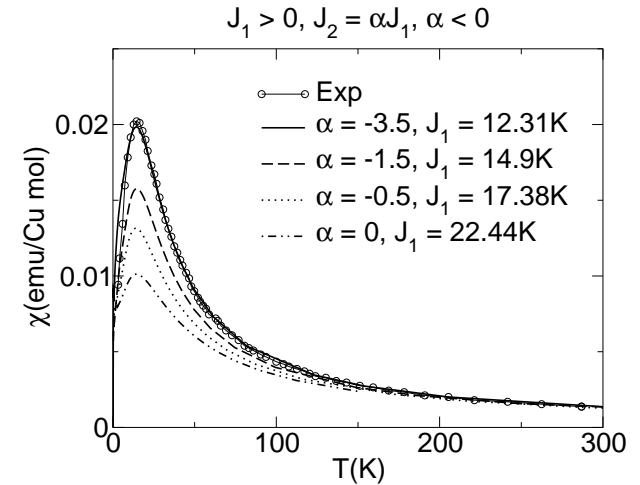


FIG. 9: Comparison of the TMRG results for the susceptibility in the AF-F case with the experimental measurement in Ref. 14.

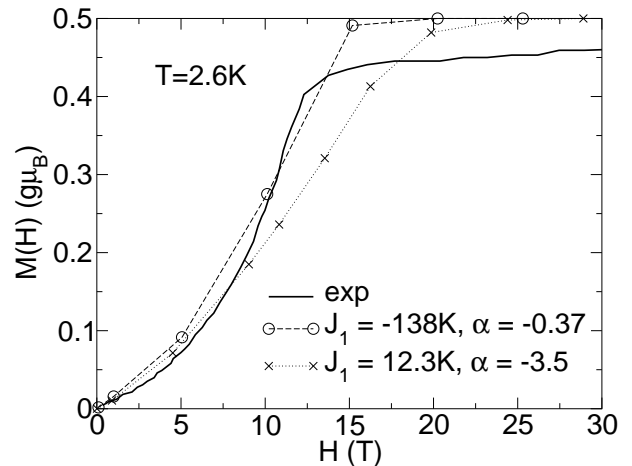


FIG. 10: Comparison of the TMRG results for the magnetization in the F-AF (circles) and AF-F (crosses) cases with the experimental measurement in Ref. 14.

also Fig. 10.)

We also calculated the field dependence of the magnetization for the two cases: $J_1 = -138$ K, $\alpha = -0.37$; and $J_1 = 12.3$ K, $\alpha = -3.5$, to verify further if the only J_1 - J_2 model is sufficient to describe the behaviors of the compound. We find the anomalous slow saturation of the magnetization cannot be reproduced either, and the result for the AF-F case seems worse.

From the TMRG numerical results on the J_1 - J_2 model and the comparison made with the experiment, we feel that only the NN and NNN interactions can not describe the properties of Rb₂Cu₂Mo₃O₁₂ satisfactorily, although a model based on the F-AF interactions seems to be an appropriate starting point.

The above facts reveal the complexity of the interac-

tions underlying the edge-sharing copper oxides. On one hand, due to the strong electron correlations in these so-called Mott insulators, very limited information on the electronic structure can be obtained reliably. This makes it difficult to calculate accurately the superexchange interaction. For instance, based on a three-band Hubbard Hamiltonian and cluster calculation, the NN and NNN interaction J_1 , J_2 for Li_2CuO_2 were obtained as $J_1 = -100$ K, $J_2 = 62$ K ($\alpha = -0.62$).¹³ The results of the quantum chemical calculation were given as $J_1 = -142$ K, $J_2 = 22$ K ($\alpha = -0.15$).⁴¹ On the other hand, because the NN coupling in edge-sharing copper oxides is extremely small, other interactions, such as quantum frustrations, weak interchain correlations, and anisotropies can all have a chance to play an unnegeigible role in determining the phase and behavior of the system. They are also closely related to the lattice structures and chemical compositions. These combined effects make any reasonable analysis intricate. In order to quantitatively recover the experimental data and various magnetic orders at low temperatures, more parameters are needed. This brings some “flexibility” to the theory. For instance, the broadening of the magnetic excitations found in $\text{Ca}_2\text{Y}_2\text{Cu}_5\text{O}_{10}$ requires the introduction of the antiferromagnetic interchain interactions and anisotropies for superexchange interactions.⁴² In order to understand the helicoidal magnetic order in NaCu_2O_2 , four parameters including frustrated longer-range exchange interactions are needed.²¹ However, we wish to emphasize here that accurate knowledge on the behavior of model 2, especially at low-temperature region, is indispensable in understanding the properties of these materials.

In conclusion, we go back to the compound $\text{Rb}_2\text{Cu}_2\text{Mo}_3\text{O}_{12}$ and take a closer look at the lattice structure of $\text{Rb}_2\text{Cu}_2\text{Mo}_3\text{O}_{12}$. Since the nearest neighbor Cu-Cu bond has two slightly alternating configurations by turns, the chain is distorted into a zigzag shape (See Fig. 1 in Ref. 14). Additional antisymmetric exchange interactions, such as Dzyaloshinskii-Moriya (DM)⁴³ or anisotropic interactions,⁴⁴ together with an alternating g tensor, should become more important than in a straight-line chain. As discussed by Dzyaloshinskii and Moriya⁴³ for the magnetic crystals with lower symmetries, the effect of this antisymmetric exchange should become more manifest than the exchange anisotropy. The magnitude of this interaction is estimated as

$$D \sim (\Delta g/g) J, \quad (13)$$

and the usual term of DM interaction can be expressed as

$$H_{\text{DM}} = \sum_j \mathbf{D}_j \cdot (\mathbf{S}_j \times \mathbf{S}_{j+1}). \quad (14)$$

Because of the alternating g tensor and the DM interaction, an external uniform magnetic field can induce an effective staggered field. If \mathbf{D}_j takes the form $(-1)^j \mathbf{D}$, as it should be in the present case, the transverse component of the staggered field, which is perpendicular to the uniformly applied field, becomes dominant. For the $S = 1/2$ Heisenberg antiferromagnetic chain, a gap is generated by a staggered field,⁴⁵ and the magnetization becomes gradually saturated for large fields.⁴⁶ The similar mechanism may also work for the F-AF case. A combination with the frustration effect caused by the NNN J_2 make the situation more interesting.

Recently, it was suggested that for $\alpha < -0.38$, there exists an incommensurate-commensurate transition at some critical field in the magnetization process.⁴⁷ The sharp increase up to $M \simeq 0.4$ at $B \simeq 14$ T and the following gradual saturation found in the experiment is argued to be connected to this phase transition.

V. SUMMARY

In this paper, we explored the properties of the zigzag spin chain with different combinations of ferro- and antiferromagnetic interactions between the NN and NNN sites. The existence of the gap in the F-AF case and the nonexistence of the gap in the AF-F case were discussed. Thermodynamic properties of the zigzag spin chain in various phases were studied by using the TMRG method. The obtained results were used to compare with the experimental data from $\text{Rb}_2\text{Cu}_2\text{Mo}_3\text{O}_{12}$. We pointed out that for such edge-sharing copper oxide chains, besides the NN and NNN couplings, more ingredients, such as the interchain or DM exchange interactions, may be important in these materials.

Acknowledgments

This work was supported by the National Natural Science Foundation of China.

¹ H. A. Bethe, Z. Phys. **71**, 205 (1931).

² F. D. M. Haldane, Phys. Lett. **83A**, 464 (1983); **50**, 1153 (1983); J. Appl. Phys. **57**, 3359 (1985).

³ M. Hagiwara, K. Katsumata, I. Affleck, B. I. Halperin, and J. P. Renard, Phys. Rev. Lett. **65**, 3181 (1990); O. Golinelli, T. Jolicoeur, and R. Lacaze, Phys. Rev. B **50**, 3037 (1994); D.C. Cabra, P. Pujol, and C. von Reichen-

bach, *ibid.* **58**, 65 (1998).

⁴ F. D. M. Haldane, Phys. Rev. B **25**, R4925 (1982); **26**, 5257 (1982).

⁵ S. R. White and I. Affleck, Phys. Rev. B **54**, 9862 (1996).

⁶ K. Okamoto and K. Nomura, Phys. Lett. A **169**, 433 (1992); S. Eggert, Phys. Rev. B **54**, R9612 (1996).

⁷ C. K. Majumdar and D. K. Ghosh, J. Math. Phys. **10**,

1388 (1969); **10**, 1399 (1969).

⁸ B. S. Shastry and Bill Sutherland, Phys. Rev. Lett. **47**, 964 (1981).

⁹ T. Tonegawa and I. Harada, J. Phys. Soc. Jpn. **58**, 2902 (1989).

¹⁰ C. Itoi and S. Qin, Phys. Rev. B **63**, 224423 (2001).

¹¹ T. Hamada, J. Kane, S. Nakagawa, and Y. Natsume, J. Phys. Soc. Jpn. **57**, 1891 (1988).

¹² N. Motoyama, H. Eisaki, and S. Uchida, Phys. Rev. Lett. **76**, 3212 (1996).

¹³ Y. Mizuno, T. Tohyama, S. Maekawa, T. Osafune, N. Motoyama, H. Eisaki, and S. Uchida, Phys. Rev. B **57**, 5326 (1998).

¹⁴ M. Hase, H. Kuroe, K. Ozawa, O. Suzuki, H. Kitazawa, G. Kido, and T. Sekine, Phys. Rev. B **70**, 104426 (2004).

¹⁵ M. Matsuda, K. Katsumata, K. M. Kojima, M. Larkin, G. M. Luke, J. Merrin, B. Nachumi, Y. J. Uemura, H. Eisaki, N. Motoyama, S. Uchida, and G. Shirane, Phys. Rev. B **55**, R11953 (1997).

¹⁶ M. Hase, I. Terasaki, and K. Uchinokura, Phys. Rev. Lett. **70**, 3651 (1993).

¹⁷ M. Matsuda and K. Katsumata, J. Magn. Magn. Mater. **177**, 683 (1998).

¹⁸ M. Matsuda, K. Katsumata, T. Yokoo, S. M. Shapiro, and G. Shirane, Phys. Rev. B **54**, R15626 (1996).

¹⁹ H. Ohta, N. Yamauchi, T. Nanba, M. Motokawa, S. Kawamata, and K. Okuda, J. Phys. Soc. Jpn. **62**, 785 (1993).

²⁰ T. Masuda, A. Zheludev, A. Bush, M. Markina, and A. Vasiliev, Phys. Rev. Lett. **92**, 177201 (2005).

²¹ L. Capogna, M. Mayr, P. Horsch, M. Raichle, R. K. Kremer, M. Sofin, A. Maljuk, M. Jansen, and B. Keimer, Phys. Rev. B **71**, 140402(R) (2005).

²² R. J. Bursill, T. Xiang, and G. A. Gehring, J. Phys.: Condens. Matter **8**, L583 (1996).

²³ X. Wang and T. Xiang, Phys. Rev. B **56**, 5061 (1997).

²⁴ T. Xiang and X. Wang, in *Density-Matrix Renormalization: A New Numerical Method in Physics*, edited by I. Peschel, X. Wang, M. Kaulke, and K. Hallberg (Springer, New York, 1999), pp. 149-172.

²⁵ D. Allen and D. Sénéchal, Phys. Rev. B **55**, 299 (1997).

²⁶ I. Affleck, in *Field Theory Methods and Quantum Critical Phenomena*, Proceedings of the Les Houches Summer School of Theoretical Physics, XLIX (Elsevier, New York, 1989).

²⁷ A. A. Nersesyan, A. O. Gogolin, and F. H. L. Essler, Phys. Rev. Lett. **81**, 910 (1998).

²⁸ D. C. Cabra, A. Honecker, and P. Pujol, Eur. Phys. J. B **13**, 55 (2000).

²⁹ A. V. Chubukov, Phys. Rev. B **44**, R4693 (1991).

³⁰ E. H. Lieb, T. Schultz, and D. J. Mattis, Ann. Phys. (N. Y.) **16**, 407 (1961); I. Affleck and E. H. Lieb, Lett. Math. Phys. **12**, 57 (1986).

³¹ R. Bursill, G. A. Gehring, D. J. J. Farnell, J. B. Parkinson, T. Xiang, and Chen Zeng, J. Phys.: Condens. Matter **7**, 8605 (1995).

³² D. Allen, F. H. L. Essler, and A. A. Nersesyan, Phys. Rev. B **61**, 8871 (2000).

³³ A. A. Aligia, C. D. Batista, and F. H. L. Essler, Phys. Rev. B **62**, 3259 (2000).

³⁴ A. Klümper and D. C. Johnston, Phys. Rev. Lett. **84**, 4701 (2000).

³⁵ S. Thanos and P. Moustanis, Physica A **271**, 418 (1999).

³⁶ F. Heidrich-Meisner, A. Honecker, and T. Vekua, Phys. Rev. B **74**, 020403(R) (2006).

³⁷ E. Lieb and D. Mattis, J. Math. Phys. **3**, 749 (1962).

³⁸ J. C. Bonner and M. E. Fisher, Phys. Rev. **135**, A640 (1964).

³⁹ S. F. Solodovnikov and Z. A. Solodovnikova, Zh. Strukt. Khim. **38**, 914 (1997) [J. Struct. Chem. **38**, 765 (1997)].

⁴⁰ M. Matsuda, K. Kakurai, J. E. Lorenzo, L. P. Regnault, A. Hiess, and G. Shirane, Phys. Rev. B **68**, 060406(R) (2003).

⁴¹ C. de Graaf, I. de P.R. Moreira, F. Illas, Ó. Iglesias, and A. Labarta, Phys. Rev. B **66**, 014448 (2002).

⁴² M. Matsuda, H. Yamaguchi, T. Ito, C. H. Lee, K. Oka, Y. Mizuno, T. Tohyama, S. Maekawa, and K. Kakurai, Phys. Rev. B **63**, 180403(R) (2001).

⁴³ I. Dzyaloshinskii, J. Phys. Chem. Solids **4**, 241 (1958); T. Moriya, Phys. Rev. B **120**, 91 (1960).

⁴⁴ V. Kataev, K.-Y. Choi, M. Grüninger, U. Ammerahl, B. Büchner, A. Freimuth, and A. Revcolevschi, Phys. Rev. Lett. **86**, 2882 (2001).

⁴⁵ M. Oshikawa and I. Affleck, Phys. Rev. Lett. **79**, 2883 (1997); I. Affleck and M. Oshikawa, Phys. Rev. B **60**, 1038 (1999).

⁴⁶ J. Z. Zhao, X. Q. Wang, T. Xiang, Z. B. Su, and L. Yu, Phys. Rev. Lett. **90**, 207204 (2003).

⁴⁷ D. V. Dmitriev and V. Ya. Krivnov, Phys. Rev. B **73**, 024402 (2006).